LA-UR-14-21946
Approved for public release; distribution is unlimited.

Title: Ultra-High Gradient Quadrupoles and Lens Length Scaling

Author(s): Walstrom, Peter L.

Intended for: Internal LANL use, collaboration with SLAC on electron radiography, etc.

Issued: 2014-03-24

Ultra-High Gradient Quadrupoles and Lens Length Scaling

P. L. Walstrom
March 22, 2014

In order to achieve very high field gradients in very small-bore small-bore quadrupole magnets, use of permanent-magnet quadrupoles (PMQs) is the only practical approach. The gradient-length product for a Halbach-type PMQ of rectangular cross section is

$$GL_{\text{eff}} = 2 f_{\text{s}} B_{\text{r}} L \left(\frac{1}{a_1} - \frac{1}{a_2} \right),$$

where f_s is a factor less than unity that takes into account the reduction in gradient due to the finite number of segments, B_r is the remanent field of the permanent-magnet material, L is the axial length of the magnet, a_1 is the inner radius, and a_2 is the outer radius. If we take f_s=0.8, B_r=1.0, a_1=4 mm, and a_2=20 mm, we get G_{eff}=320 T/m. A B_r value of 1.0 T is typical of samarium-cobalt PM material. Note that f_s approaches a limiting value of 1 as the number of segments in the PMQ increases. With fixed a_1, higher gradients can be achieved by increasing B_r and a_2. With infinite a_2, the limiting G in the above example is 400 T/m instead of 320 T/m. The remanent field B_r can be increased to 1.2 to 1.3 T by use of neodymium-iron-boron PM material, but then the radiation sensitivity is much greater. Some improvement in B_r together with radiation resistance may be available by use of praeseodymium-based PM material, but these PM materials are not readily available commercially.

As a rule of thumb, in a magnetic quadrupole lens, we set the inner radius of the quadrupoles equal to three times the radius of the desired field of view (FOV). This rule of thumb has the hidden assumption that scattering and matching angles do not dominate the field of view. With this criterion, the above 320 T/m quadrupoles allow a field-of-view diameter of approximately 2.7 mm. This should be checked with tracking studies.

Since the permanent-magnet segments must be contained by a cylindrical non-magnetic can, the physical outer radius of the 320 T/m PMQs with a_2=20 mm is about 21 mm.

In order to check scaling of total lens length with quadrupole gradient, two series of single-stage magnifying lenses for 12 GeV electrons were designed, using various quadrupole lengths and gradients. For the larger-bore magnets in the two series, conventional magnets could be used. Marylie with its hard-edge quadrupole model and fit loops was used to determine quadrupole strengths and final drift length. In view of the relatively large length/bore-radius ratios of the quadrupoles, this is a good approximation and real PMQ lengths and spacings should be close to the hard-edge values. Every lens had a magnification of -10. The lenses were all of the so-called Russian quadruplet type. The lengths of the inner two quadrupoles (B quadrupoles) were taken to be twice those of the outer two quadrupoles (A quadrupoles). In Series 1, the initial drift and quadrupole spacings were taken to be equal to the lengths of the B quadrupoles (see Fig. 1). In Series 2, the initial drift was set to be equal to the length of the A quadrupoles (see Fig. 2). For each lens in both series, the object standoff, quadrupole lengths and spacing were fixed and the final drift L was varied along with the gradients G_A and G_B to simultaneously focus the lens and give a magnification of -10 in both the x and y planes. With B quadrupoles exactly twice as long as the A quadrupoles, the required B gradients were a little larger than the A gradients. The data for the two series of lenses are given in Tables

I and II. Distances are in meters and gradients in T/m. Note that if we keep B_r, f_s, and a_1/a_2 constant, a_1 and the available field-of-view diameter both vary inversely with gradient. That is, with the highest gradient in the Table I, 556.6 T/m, the available FOV diameter is about 1.5 mm, while with the lowest gradient, 15.46 T/m, the available FOV diameter is about 55 mm. We can also see from Tables I and II that the product $(G_{av})^{1/2}d$ and the ratio L_{tot}/d are constant through the series.

Fig. 3 is a plot of the values of total lens length L_{tot} *vs*. the inverse square root of the quadrupole gradient from Tables I and II. As can be seen, the dependence is perfectly linear. Also, doubling the relative object standoff distance has only a small effect on lens length and quadrupole gradients.

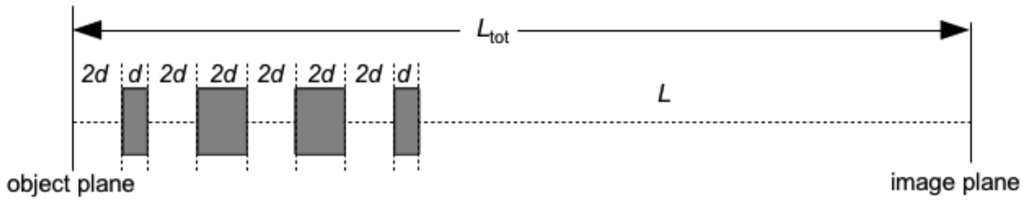

Fig. 1. Series 1 lens layout and nomenclature. The standoff distance 2*d* was set equal to the length 2*d* of the two longer quadrupoles (B quadrupoles).

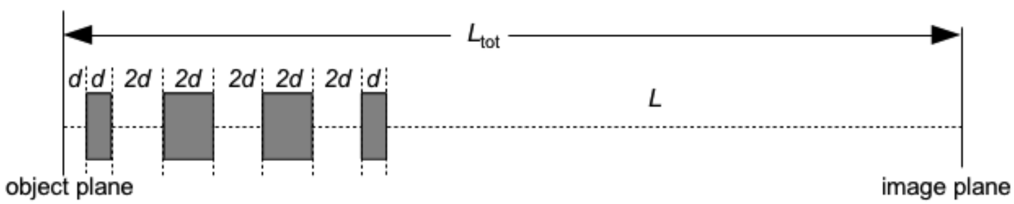

Fig. 2. Series 2 lens layout and nomenclature. The standoff distance *d* was set equal to the length *d* of the two shorter quadrupoles (A quadrupoles.

Table I. Series 1 of Lenses with Increasing Gradients

d	L	G_A	G_B	$\bar{G}$	$\bar{G}^{-1/2}$	L_{tot}	T_{116}	T_{126}	T_{336}	T_{346}
0.6	52.70	15.08	15.85	15.46	0.2543	61.10	-13.84	-147.7	-15.25	-75.55
0.4	35.13	33.92	35.65	34.79	0.1696	40.73	-13.84	-98.49	-15.25	-50.37
0.3	26.35	60.30	63.38	61.84	0.1272	30.55	-13.84	-73.87	-15.25	-37.78
0.18	15.81	167.5	176.1	171.8	0.0763	18.33	-13.84	-44.32	-15.25	-22.67
0.15	13.18	241.2	253.5	247.4	0.0636	15.28	-13.84	-36.93	-15.25	-18.89
0.132	11.59	311.5	327.4	319.4	0.0560	13.44	-13.84	-32.50	-15.25	-16.62
0.10	8.783	542.7	570.4	556.6	0.0424	10.18	-13.84	-24.62	-15.25	-12.59

Table II. Series 2 of Lenses with Increasing Gradients

d	L	G_A	G_B	$\bar{G}$	$\bar{G}^{-1/2}$	L_{tot}	T_{116}	T_{126}	T_{336}	T_{346}
0.6	48.62	16.68	16.83	16.75	0.2443	56.42	-11.63	-147.7	-13.38	-63.10
0.4	32.41	37.52	37.87	37.70	0.1629	37.61	-11.63	-98.08	-13.38	-42.07
0.18	14.59	185.3	187.0	186.2	0.0733	16.93	-11.63	-44.15	-13.38	-18.93

0.10	8.1035	600.4	606.0	603.2	0.0407	9.403	-11.63	-24.52	-13.38	-10.52

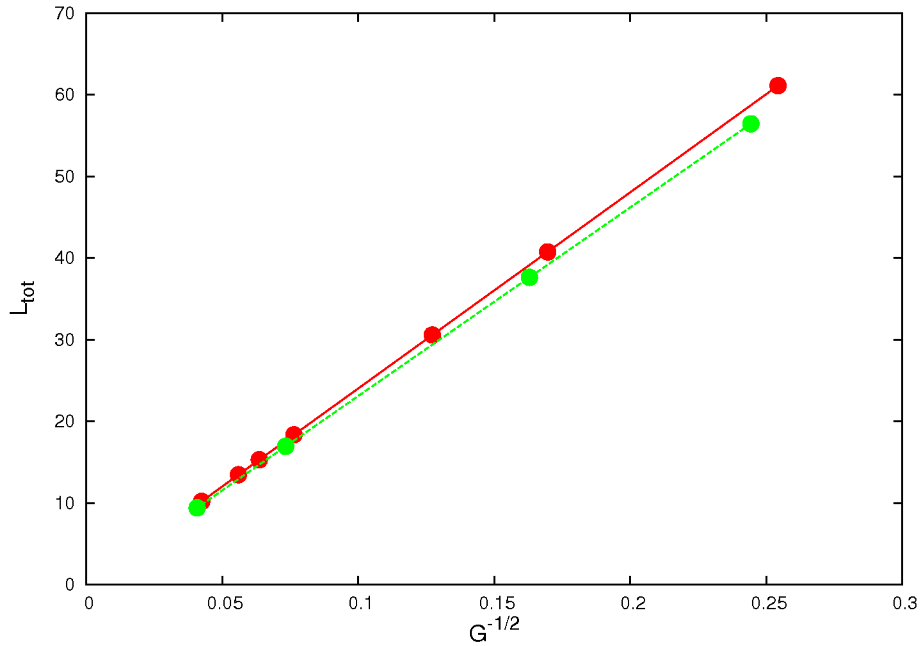

Fig. 3. Plot of total lens length *vs*. the inverse square root of the average quadrupole gradient. Red curve: Series 1 lenses; green curve: Series 2 lenses.

In addition to total lens length, another concern is the magnitude of the second-order chromatic aberration coefficients T_{116}, T_{126}, T_{336}, and T_{346}. These coefficients are plotted against the inverse square root of the average gradient in Fig. 4.

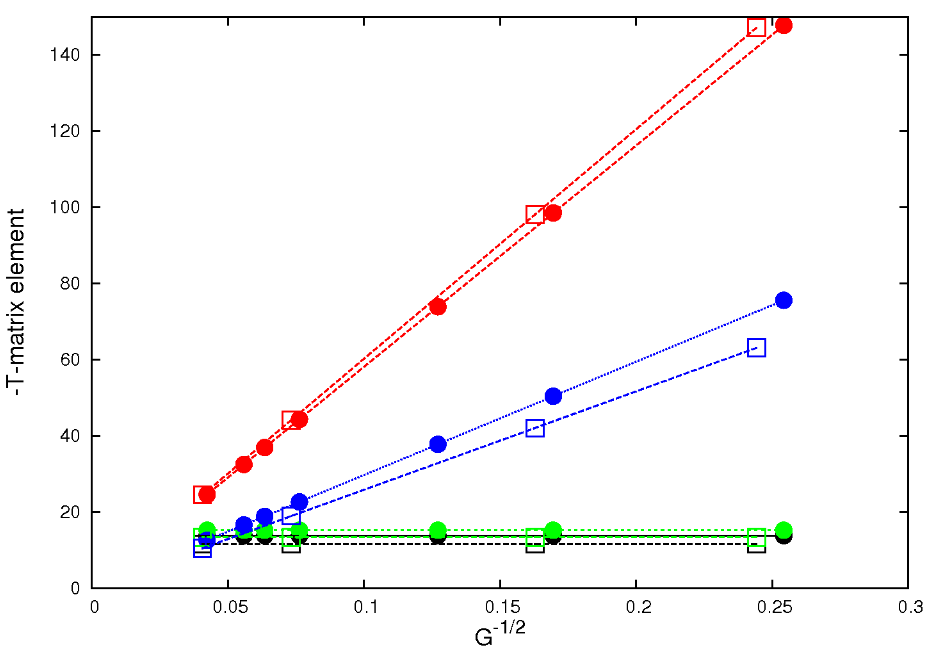

Fig. 4. Plot of second-order chromatic-aberration coefficients *vs*. the inverse square root of the average quadrupole gradient. Red curves: T_{126} ; blue curves: T_{346}; black curves: T_{116}; green curves: T_{336}. Solid circles: Series 1 lenses; open squares: Series 2 lenses.
From the tables and from Fig. 4 it can be seen that T_{126} and T_{346} are proportional to both lens length and to the inverse square root of G, while T_{116} and T_{336} are constant throughout a series. It can also be seen that increasing the relative standoff distance by a factor of two has only a small effect on chromatic aberrations. Note that the effective coefficients would be those of the tables divided by the magnification (10 in this case).

The fact that T_{116} and T_{336} are constant, while T_{126} and T_{346} decrease as gradients increase means that the matching coefficients $k_x = - T_{116} / T_{126}$ and $k_y = - T_{336} / T_{346}$ increase as gradients increase. This implies that stronger quadrupole gradients will be required in the matching section for the shorter lenses with higher quadrupole gradients. Based on previous experience, geometric aberration coefficients will be greater in the shorter lenses, but this should be offset by the smaller field of view and angular spread in experiments that use the high-gradient, short lenses. This needs to be checked.